Energy Efficient Single Stack Exhaust Fan Systems (E^3S^3F)

Gang Wang
Visiting Research Scholar
College of Engineering and Technology
University of Nebraska – Lincoln

Mingsheng Liu
Associate Professor
College of Engineering and Technology
University of Nebraska – Lincoln

ABSTRACT

This paper first investigates the fan energy performance of a constant air volume exhaust system. Two single stack energy efficient exhaust fan systems (E^3S^3F)[1] are presented. The E^3S^3F-I has the static pressure sensor located at the inlet of the exhaust fan. It has been found to consume up to 15% less fan power than conventional constant air volume exhaust systems. The E^3S^3F–II uses a variable speed device to maintain the static pressure at the entrance of the stack. It consumes up to 60% less fan power than conventional constant volume exhaust systems.

INTRODUCTION

Laboratory exhaust systems provide the required pressure difference for fume hood operation and prevent toxic contamination of the building and its surroundings. Since all fume hood and exhaust devices are seldom used simultaneously at full capacity, there are opportunities to conserve energy and to decrease the system capacity. The potential HVAC energy savings has been investigated extensively in the past 20 years [Maust and Rundquist 1987, Neuman and Guven, 1988, Brown 1993, and Doyle et al. 1993]. Variable volume fume hood systems and heat recovery systems have significantly decreased HVAC energy consumption in many applications.

The required capacity of a manifolded pressure-independent exhaust system could be greatly reduced by employing the concept of the overall system usage factor. This usage factor has been analyzed and measured [Moyer and Dungan 1987, Rabiah and Wellenbach 1993, and Varley 1993]. However, design engineers are reluctant to adopt the concept since the mechanical system cannot bear the uncertainty of a statically determined usage factor. The exhaust fan and ductwork are still designed based on the maximum possible exhaust airflow.

Stack height is a critical issue in preventing local toxic air contamination. Design rules and criteria have been developed based on recent research and study [Changnon 1966, Rock and Moylan 1999, Wilson and Winkel 1982, and Wilson and Ackerman 1998]. The stack must be 10 feet above any adjacent roofline and at least one stack diameter above any architectural screen in order to prevent exhaust contamination from re-circulating into the building [ASHRAE 1999]. The stack must also project 10 feet above the roof to protect roof workers [AIHA 1992]. If a stack is designed shorter than 10 feet due to architectural requirements, both the volumetric flow and the discharge velocity must be increased to increase the discharge momentum.

The exit velocity is required to be 2,000 fpm or higher in order to provide adequate plume rise and jet dilution and to avoid stack-wake downwash [AIHA 1992]. To prevent condensed moisture from draining down the stack and rain from entering the stack, the air velocity in the stack must be 2,500 fpm or higher [AIHA 1992]. If the air velocity is higher than 3,000 fpm, noise and vibration from the exhaust fan become an important concern. Therefore, most exhaust systems are designed as constant volume systems with exit velocity of 3,000 fpm. A constant speed fan is typically used. When the airflow from the fume hood is less than the design volume, a make-up air damper at the inlet of the fan is used to maintain the static pressure set point of the fume hood system and maintain the minimum required stack exit velocity. When the make-up air damper is open, both fan airflow and power consumption are higher than at the design values. Since the total exhaust airflow from fume hoods rarely reaches the design value for either variable air volume or constant volume fume hood systems, the exhaust fan power is higher than the design value most, if not all, of the time.

This paper first investigates the fan energy performance of a constant air volume exhaust system. Two energy efficient single stack exhaust fan systems (E^3S^3F) also are presented.

[1] Patent application pending

CONSTANT AIR VOLUME EXHAUST SYSTEM

Figure 1 shows a schematic diagram of constant air volume exhaust systems. A constant speed fan and a makeup air damper are used to maintain the stack design velocity and negative static pressure for the fume hood system.

The makeup air damper is attached to the inlet of the fan (point B). The static pressure sensor (sensor A) is located at the main exhaust air duct, where the nearest fume hood is attached to the exhaust system. The static pressure set point is negative. The absolute value should be higher than or equal to the pressure head required by the fume hood operation. The set point is assumed to be constant in this study.

Under design conditions, the fan airflow is equal to the fume hood airflow. The makeup damper is closed. When the fume hood airflow is less than the design value, the controller modulates the makeup damper so as to maintain the static pressure set point. When the makeup air damper is open or partially open, the airflow through the fan is higher than the design flow, because the exhaust system now has a lower overall flow resistance.

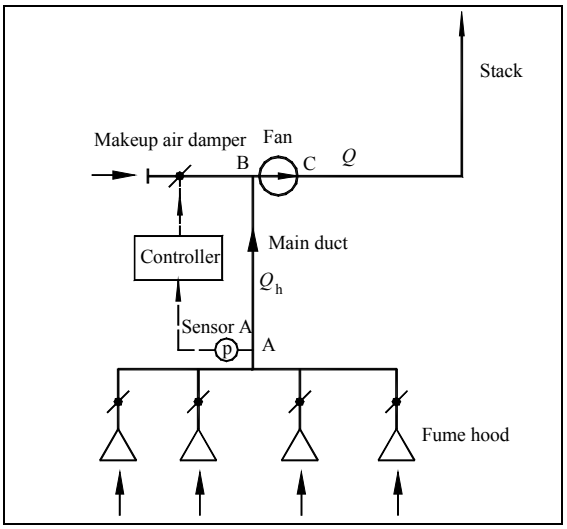

Figure 1. Schematic Diagram of Constant Air Volume Exhaust Systems

The fan head is the sum of the static pressure at point A, duct pressure loss from the static pressure sensor location (point A) to the stack exit, and the dynamic head difference between the stack exit and the location of the static pressure sensor.

$$H = |P_1| + \Delta P_2 + \Delta P_3 + \Delta P_d \qquad (1)$$

The static pressure set point is constant; the duct pressure loss is a function of the airflow through each section. The dynamic head difference is relatively small and is ignored in this study.

To introduce these conditions into Equation 1:

$$\overline{H} = x_1 + x_2 \cdot (\overline{Q}_h)^2 + x_3 \cdot (\overline{Q})^2 \qquad (2)$$

where:

$\overline{H} = H / H_d$

$\overline{Q} = Q / Q_d$

$\overline{Q}_h = Q_h / Q_d$

$x_1 = |P_{1,d}| / H_d$

$x_2 = \Delta P_{2,d} / H_d$

$x_3 = \Delta P_{3,d} / H_d$

The fan airflow can be determined by combining the fan curve and the duct system curve (Equation 2). Figure 2 shows a dimensionless fan curve for typical centrifugal fans. The fan power and fan head ratios are expressed as functions of the airflow ratio. The reference point is the fan design working point, where the fan has its highest efficiency. The fan airflow ratio is the ratio of the airflow to the design airflow. The fan head ratio is the ratio of the fan head to the design head. The fan power ratio is the ratio of actual power to design power.

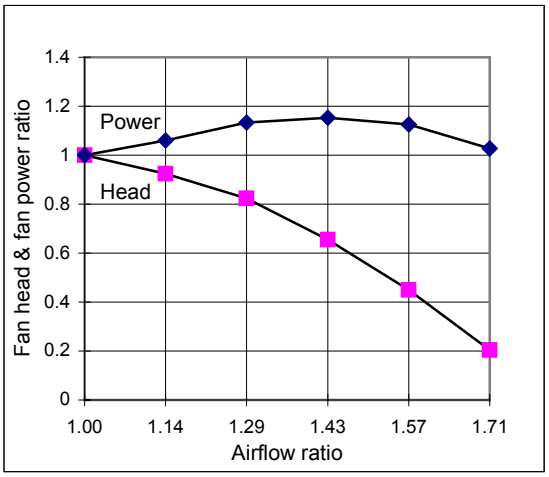

Figure 2. Fan Head and fan Power Ratio Versus the Airflow Ratio for Typical Centrifugal Fans (The reference point has the maximum efficiency)

The fan head and fan power are regressed as functions of the fan airflow:

$$\overline{H} = 0.0978 + 2.1521\overline{Q} - 1.2964\overline{Q}^2 + 0.0447\overline{Q}^3 \quad (3a)$$

$$\overline{W} = 2.1314 - 4.001\overline{Q} + 4.1416\overline{Q}^2 - 1.2774\overline{Q}^3 \quad (3b)$$

The ratio of stack pressure loss and the fume hood pressure loss (x_3 to x_1) can be considered a fixed number (0.5). The fan power is, then, a function of the fume hood flow ratio and the pressure loss ratio of the main duct from the static pressure sensor to the fan inlet. In this study, the pressure loss ratio is defined as the ratio of the main duct pressure loss to the fixed pressure need (x_2 to (x_1+x_3)).

The fan airflow, head, and power consumption are simulated under different fume hood flow ratios ($\overline{Q}_h$) and pressure loss ratios (x_2 / (x_1+x_3)).

Figure 3 illustrates the simulated fan airflow. The fan airflow increases as the fume hood airflow decreases and/or the main duct pressure-loss fraction increases. Under partial fume hood airflow, actual fan airflow could be up to 42% higher than design airflow.

Figure 4 presents the simulated fan head. The fan head decreases as the fume hood airflow decreases and/or the main duct pressure loss fraction increases. When the fume hood airflow is 10% of the design value and the pressure loss ratio is 1, the fan head can be as low as 67% of the design head. The excessive airflow and low fan head is caused by low resistance when the make-up air damper is open.

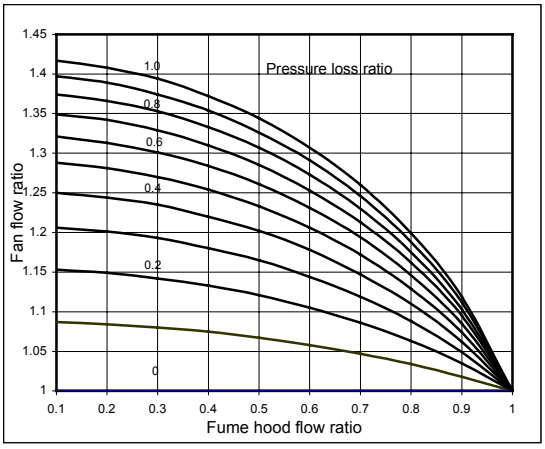

Figure 3. Simulated Fan Airflow Ratio Versus the Fume Hood Airflow Ratio Under Different Pressure Loss Ratios

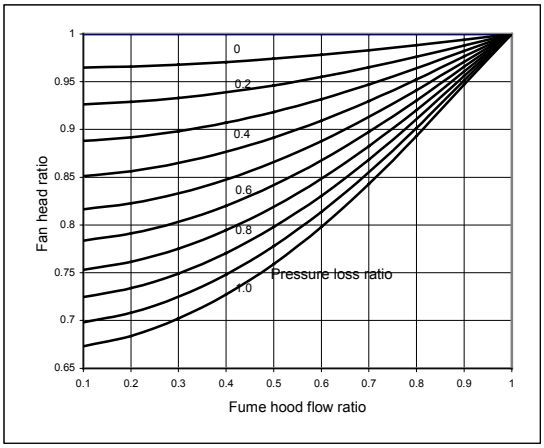

Figure 4. Simulated Fan Head Ratio Versus the Fume Hood Airflow Ratio Under Different Pressure Loss Ratios

Figure 5 shows the simulated fan power. The fan power is higher than the design value when the fume hood airflow is lower than the design value and main duct pressure loss is higher than zero. The lower the fume hood airflow, the higher the fan power. For the same fume hood airflow, excessive fan power increases as the main duct pressure loss ratio increases. Actual fan power can be up to 15% higher than the design fan power for a typical constant volume exhaust system.

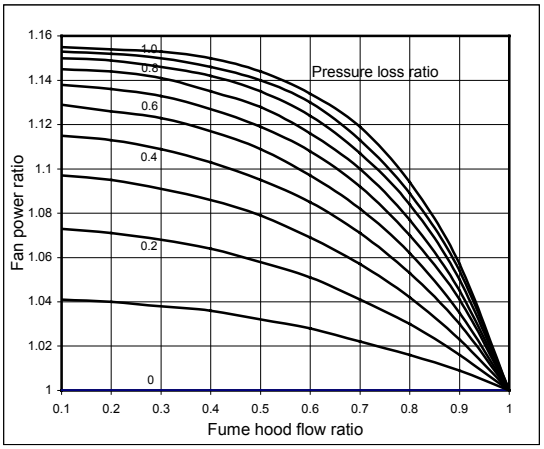

Figure 5. Simulated Fan Power Ratio Versus the Fume Hood Airflow Ratio Under Different Pressure Loss Ratios

E^{3}S^{3}F-I

The excessive fan power in the base system is caused by excessive airflow under partial fume hood airflow. To eliminate the excessive fan power, the static pressure sensor (sensor A) is relocated to the inlet of the fan.

Figure 6 shows a schematic diagram of the E^3S^3F-I. A constant static pressure at point B is maintained by the makeup air damper position, regardless of the fume hood airflow. The fan has a constant fan head, airflow and power consumption under all fume hood airflow conditions.

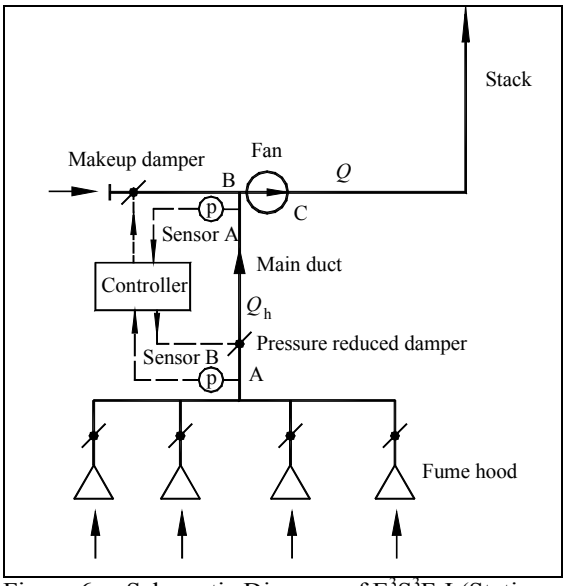

Figure 6. Schematic Diagram of E^3S^3F-I (Static pressure sensor is relocated at the fan inlet)

The static pressure at the fume hood varies with the fume hood airflow. The static pressure at the original sensor location (point A) is expressed by Equation 4.

$$\frac{P_1}{P_1'} = 1 + \frac{x_2}{x_1}(1 - \overline{Q}_h^{\,2}) \qquad (4)$$

The static pressure variation at the original sensor location is simulated under different fume hood airflow ratios and main duct pressure loss ratios. The static pressure variation is expressed as the ratio of the static pressure to the initial design set point. The results are presented in Figure 7. The negative pressure increases as the fume hood airflow ratio decreases and the duct pressure loss ratio increases. The actual static pressure P_1 can be up to 2.5 times the design value P_1'.

Excessive static pressure can create noise problems. To solve noise problems, a damper could be installed in the main duct to maintain the original set point of the static pressure (See Figure 6 for detail). When the makeup air damper is partially open, the pressure-reducing damper would be modulated to maintain the original static pressure.

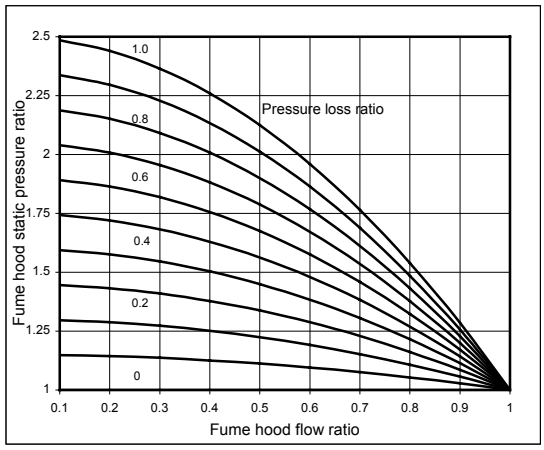

Figure 7. Simulated Static Pressure Ratio for E^3S^3F-I: Static pressure sensor is relocated at the inlet of the fan

Figure 8 compares the fan power of the E^3S^3F-I with the base system. The fan power reduction ratio is defined as the ratio of fan power reduction to design fan power. The lower the fume hood airflow, the greater the fan power reduction. For the same fume hood airflow, the energy savings increases as the main duct pressure loss fraction increases. The sensor relocation can reduce fan power by up to 15%.

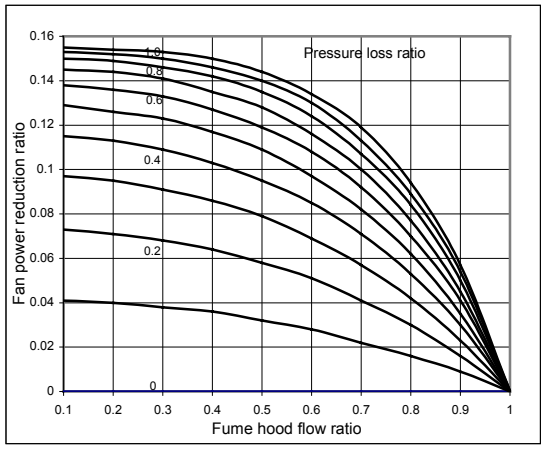

Figure 8. Simulated Fan Power Reduction Ratio Versus the Fume Hood Airflow Ratio Under Different Duct Pressure Loss Ratios

E^3S^3F-II

E^3S^3F-I maintains fan power at the design value under partial fume hood flow rates. The simulation results show an excessive pressure difference for the fume hood. This indicates inefficiency within the

system. To improve the energy efficiency, E^3S^3F-II uses a variable speed device (VSD) for the fan. Figure 9 presents the schematic diagram of the E^3S^3F-II.

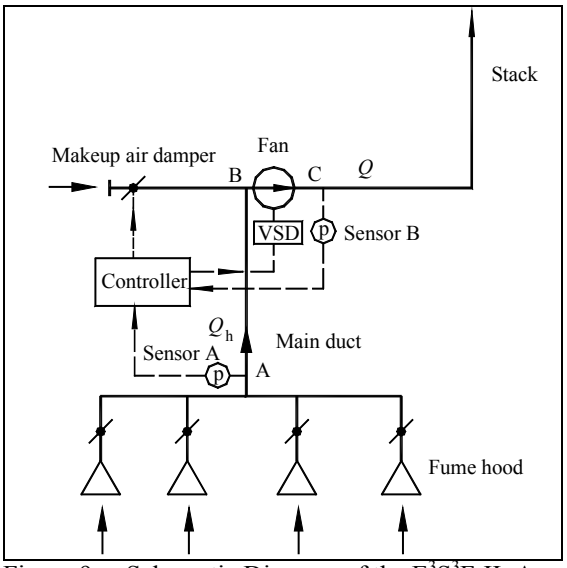

Figure 9. Schematic Diagram of the E^3S^3F-II. A VSD is installed on the exhaust fan

In addition to the VSD, another static sensor (sensor B) is added at the outlet of the fan. The original static pressure is used in this system. The controller modulates the makeup air damper to maintain the static pressure set point at point A and modulates the fan speed to maintain the static pressure set point at point C.

The fan head is equal to the total pressure loss of the system. It is expressed by Equation 5.

$$\overline{H} = x_1 + x_2 \cdot (\overline{Q}_h)^2 + x_3 \quad (5)$$

The efficiency of the VSD is assumed to be 1 in this study. The fan efficiency under different fan speeds is determined based on fan similarity. The equivalent fan flow rate at the design fan speed can be determined based on fan head by using Equation 6.

$$\overline{HQ}_e^2 = 0.0978 + 2.1521\overline{Q}_e - 1.2964\overline{Q}_e^2 + 0.0447\overline{Q}_e^3 \quad (6)$$

The equivalent fan power is then determined using the equivalent fan flow:

$$\overline{W}_e = 2.1314 - 4.001\overline{Q}_e + 4.1416\overline{Q}_e^{\,2} - 1.2774\overline{Q}_e^{\,3} \quad (7)$$

Finally, fan power is determined by:

$$\overline{W} = \frac{\overline{W}_e}{\overline{Q}_e^3} \quad (8)$$

Figure 10 compares the simulated fan power with the base system. The fan power reduction ratio is defined as the ratio of fan power reduction to the design fan power. The lower the fume hood airflow, the greater the fan power reduction. For the same fume hood airflow, the energy savings increases as the main duct pressure loss ratio increases. The VSD installation can reduce fan power by up to 60%. For a typical constant volume exhaust system, the annual energy savings may be up to 40%.

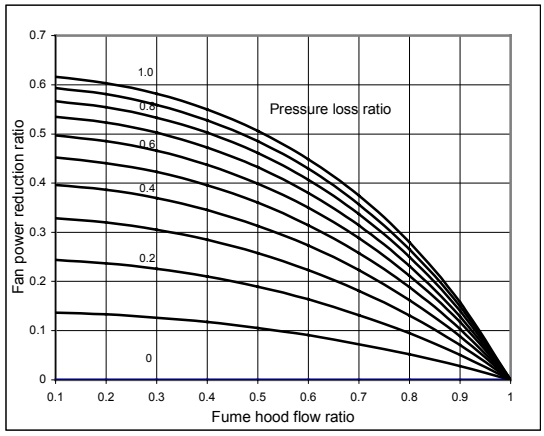

Figure 10. Simulated Fan Power Reduction Ratio Versus the Fume Hood Airflow Ratio Under Different Duct Pressure Loss Ratios

CONCLUSIONS

For a typical constant volume exhaust system under a partial fume hood load condition, the fan power is up to 15% higher than the design fan power. The excessive fan power is dependent on the fume hood airflow and the main duct pressure loss ratio. The lower the fume hood airflow and the higher the main duct pressure loss fraction, the higher the excessive fan power.

E^3S^3F-I has a static pressure sensor at the inlet of the fan. It maintains the fan power at design value under partial fume hood airflow rate. It can save up to 15% fan power compared with a conventional constant air volume exhaust system. An additional pressure-reducing damper may be required to prevent noise problems.

E^3S^3F-II uses a variable speed device to maintain the static pressure set point at the entrance of the stack, and uses a make-up air damper to maintain the

static pressure set point at the fume hood location. It consumes up to 60% less fan power than conventional constant air volume exhaust systems

NOMENCLATURE

H = fan head;
H_d = fan design head;
$\overline{H}$ = relative fan head;
Q = fan airflow;
Q_d = fan design airflow;
Q_h = hood airflow;
$\overline{Q}$ = relative fan airflow;
$\overline{Q}_e$ = ratio of the equivalent fan flow at the design fan speed to the fan design flow;
$\overline{Q}_h$ = relative hood airflow;
P_1 = static pressure at point A;
$P_{1,d}$ = design static pressure at point A;
P_1' = design static pressure of the base system;
$\overline{W}$ = relative fan power, the ratio of the fan power to the design fan power;
$\overline{W}_e$ = ratio of the equivalent fan power at the design fan speed to the fan design power;
x_1 = relative design static pressure at point A;
x_2 = relative design pressure loss in section AB;
x_3 = relative design pressure loss after the fan;
ΔP_2 = pressure loss in the main exhaust air duct (section AB);
ΔP_3 = pressure loss in the duct and stack after the fan;
ΔP_d = dynamic head difference between the stack exit and point A;
$\Delta P_{2,d}$ = design pressure loss in section AB;
$\Delta P_{3,d}$ = design pressure loss after the fan;

REFERENCES

AIHA. 1993. Laboratory ventilation. ANSI/AIHA Standard Z 9.5-93. American Industrial Hygiene Association, Fairfax, VA.

ASHRAE. 1999. HVAC Application. American Society of Heating, Refrigeration and Air-conditioning Engineering, Inc. Atlanta, GA.

Brown W. K. 1993. An Integrated approach to laboratory energy efficiency. ASHRAE Transactions 99(2).

Changnon, S. A. 1966. Selected rain-wind relations applicable to stack design. Heating Piping and Air Conditioning 38(3):93.

Doyel, D. L., R. D. Benzuly and J. M. O'Brien. 1993. Variable volume retrofit of an industrial research laboratory. ASHRAE Transactions 99(2).

Maust, J. and R. Rundquist. 1987. Laboratory fume hood systems-Their use and energy conservation. ASHRAE Transactions 93(2B).

Moyer, R. and J. Dungan. 1987. Turning fume hood diversity into energy savings. ASHRAE Transactions 93(2B).

Neuman, V. and H. Guven. 1988. Laboratory building HVAC systems optimization. ASHRAE Transactions 94(2).

Rabiah, T. M. and J. W. Wellenbach. 1993. Determining fume hood diversity factors. ASHRAE Transactions 99(2).

Rock, B. A. and K. A. Moylan. 1999. Placement of ventilation air intakes for improved IAQ. ASHRAE Transactions 105(1).

Varley, J. O. 1993. The measurement of fume hood use diversity in an industrial laboratory. ASHRAE Transactions 99(2).

Wilson, D. J. and G. Winkel. 1982. The effect of varying exhaust stack height on contaminant concentration at roof level. ASHRAE Transactions 88(1):513-33.

Wilson, D. J., I. Fabris, and M. Y. Ackerman. 1988. Measuring adjacent building effects on laboratory exhaust stack design. ASHRAE Transactions 104(2).